***Military Technical College***
***Kobry El-Kobbah,***
***Cairo, Egypt.***

***15th International Conference on Applied Mechanics and Mechanical Engineering.***

# NUMERICAL COMPUTATION OF BUOYANCY-DRIVEN FLOW AND HEAT TRANSFER IN VARIOUS ASPECT RATIOS CAVITIES FILLED WITH WATER

S. H. Hussain[1], A. K. Hussein[2,*], H. H. Al-Kayiem[3] and H. F. Oztop[4]

## ABSTRACT

Two-dimensional steady laminar natural convection in a differentially heated cavity filled with water and has various aspect ratios due to buoyancy force effect is analyzed numerically. The governing mass, momentum and energy equations are considered and a finite volume algorithm is used to capture the numerical solution. The left vertical side wall of the cavity is linearly heated while the right vertical one is maintained at constant cold temperature. The bottom wall is maintained at constant hot temperature while the top wall is considered thermally insulated. The Rayleigh number is varied from $10^3$ to $10^6$, while the cavity aspect ratio (W/H) is varied as 0.5, 1.0 and 2.0 respectively. Results are presented in the form of streamline and isotherm contours. The results of the present work explain that the natural convection phenomenon is significantly influenced by changing the cavity aspect ratio, so that when the aspect ratio is high the convection effect is week and vice versa. Also, it is found that non-uniform heating in the left vertical sidewall of the cavity plays a major role to improve the heat transfer rates. For uniform and non-uniform heating of the bottom wall and left vertical sidewall respectively, the local Nusselt number at these walls increases from its minimum value at the left edge of these walls toward maximum value at the right edge. While, the average Nusselt number for both left side and bottom walls increases with increasing of Rayleigh number.

**KEY WORDS:** Buoyancy-driven flow, CFD simulation, aspect ratio, cavity, laminar flow and linear heating.

---

1 College of Engineering, Mechanical Engineering Department, Babylon University, Babylon City, Hilla , Iraq. Email: salamphd1974@yahoo.com.

2,* College of Engineering, Mechanical Engineering Department, Babylon University, Babylon City, Hilla , Iraq. Corresponding author. E-mail address: ahmedkadhim74@yahoo.com.

3 Mechanical Engineering Department, University Teknologi Petronas, 31750 Tronoh , Perak, Malaysia. Email: hussain_kayiem@petronas.com.my.

4 Department of Mechanical Engineering, Technology Faculty, Firat University, Elazig, Turkey. Email: hfoztop1@yahoo.com.

## NOMENCLATURE

| Symbol | Description | Unit |
|---|---|---|
| g | Gravitational acceleration | $m/s^2$ |
| H | Height of the cavity | m |
| $\overline{Nu}$ | Average Nusselt number | |
| Nu | Local Nusselt number | |
| P | Dimensionless pressure | |
| p | Pressure | $N/m^2$ |
| Pr | Prandtl number | |
| Ra | Rayleigh number | |
| T | Temperature | °C |
| U | Dimensionless velocity component in x-direction | |
| u | Velocity component in x-direction | m/s |
| V | Dimensionless velocity component in y-direction | |
| v | Velocity component in y-direction | m/s |
| W | Width of the cavity | m |
| X | Dimensionless Coordinate in horizontal direction | |
| x | Cartesian coordinate in horizontal direction | m |
| Y | Dimensionless Coordinate in vertical direction | |
| y | Cartesian coordinate in vertical direction | m |

### GREEK SYMBOLS

| | | |
|---|---|---|
| α | Thermal diffusivity | $m^2/s$ |
| β | Coefficient of thermal expansion | $K^{-1}$ |
| θ | Dimensionless temperature | |
| ν | Kinematic viscosity of the fluid | $m^2/s$ |
| ρ | Density of the fluid | $kg/m^3$ |

### SUBSCRIPTS

| | |
|---|---|
| B | Bottom |
| c | Cold |
| h | Hot |
| L | Left |

## INTRODUCTION

In various thermal applications, the problems of control and measurement of heat transfer by buoyancy-driven flow (sometimes, called natural convection) is very important process. This type of flow is generated by density gradients, which in most cases arise from some imposed external heat source. In most cases, the theoretical approach is impossible; therefore experimentation (numerical or standard experimentation) is used to simulate buoyancy-driven flow problems. The heat transfer by natural convection motion was used as an important model for many

engineering purposes. For example, circulation of fluid in electronic or computer equipments, in the study of the structure of stars and planets, thermal energy storage systems, cooling of nuclear reactors and so on. Therefore, for this reason the natural convection heat transfer in cavities has received considerable attention for several years [1].Square and rectangular cavities heated and cooled on the sides continue to be the geometry of most interest. Several numerical simulations have been reported for various aspect ratios and boundary conditions. The square cavity has been registed in the literature as the most suitable case for the validation of numerical codes for thermal analysis and for physical understanding of buoyancy-driven flow in cavities. The most usual working fluids analyzed in the literature have been mainly air and water.

## LITERATURE REVIEW

Experimental and numerical investigations on natural convection heat transfer in cavities and enclosures have carried out by numerous researchers. Imberger [2] studied experimentally the steady motion of water in an enclosed rectangular cavity with differentially heated vertical end walls. The Rayleigh number was allowed to vary sufficiently to enable a study to be made of the transition from a flow driven by the vertical wall boundary layers to one sustained by a longitudinal temperature gradient in the central sections of the cavity.

Hasnaoui et al. [3] investigated by using a finite difference procedure the natural convection in an enclosed cavity with localized heating from below. The upper surface was considered cooled at a constant temperature and a portion of the bottom surface was isothermally heated while the rest of the bottom surface and the vertical walls were considered adiabatic. The effects of the thermophysical and geometrical parameters on the fluid flow and temperature fields were studied also. Moreover, the existence of multiple steady-state solutions and the oscillatory behavior for a given set of the governing parameters were demonstrated.

Braunsfurth et al. [4] presented numerical and experimental temperature profiles corresponding to laminar natural convection of liquid gallium in a rectangular cavity heated through the side walls. They concluded that at higher Grashof numbers, the two-dimensional numerical solution and the experimental data diverged from each other suggesting that three-dimensional effects became more important. Aydin and Yang [5] investigated numerically natural convection of air in a two-dimensional, rectangular enclosure with localized heating from below and symmetrical cooling from the sides. Local results are presented in the form of streamline and isotherm plots as well as the variation of local Nusselt number on the heated wall.

Kalita et al.[6] computed using an accurate higher-order compact scheme, the flow in a thermally driven square cavity with adiabatic top and bottom walls and differentially heated vertical walls for a wide range of Rayleigh numbers ($10^3$<Ra<$10^7$).They concluded that, the location of the maximum local Nusselt number at the hot wall progressively moved down as Rayleigh number increased. Also, they noticed that the boundary layer thickness was seen to progressively decrease as Rayleigh number increased.

Basak et al. [7] performed a numerical study by using a finite element method to investigate the steady laminar natural convection flow in a square cavity with uniformly and non-uniformly heated bottom wall, and adiabatic top wall maintaining constant temperature of cold vertical walls. The results indicated that the non-uniform heating of the bottom wall produced greater heat transfer rates at the center of the bottom wall than the uniform heating case for all Rayleigh numbers while the average Nusselt numbers results showed lower heat transfer rates for the non-uniform heating case.

Xin and Quere [8] simulated two-dimensional natural convection in an air-filled differentially heated cavities of aspect ratios ranging from 1 to 7 with adiabatic horizontal walls using sophisticated algorithms of stability analysis. They concluded that, when aspect ratio was increased, not only detached flow was observed at higher Rayleigh number, but also regular evolution from flows without detached flow to those with detached flow was no longer possible.

Mariani and Belo [9] studied numerically the thermal and fluid dynamics behavior of laminar natural air convection in a bi-dimensional square cavity. The square cavity had two walls heated with different temperatures and two isolated walls. The Boussinesq approximation was used with a constant Prandtl number and the numerical simulation was made up of several Rayleigh numbers. They concluded that with the growth of the Rayleigh number, there was a growth of circulation inside the cavity. Also, a clear compression of isotherms near cavity boundaries was observed.

Basak et al.[10] studied numerically by using the finite-element method the influence of uniform and non-uniform heating of wall(s) on natural-convection flow in a square cavity filled with a porous medium. In their investigation, the left vertical wall and the bottom wall were uniformly and non-uniformly heated, while the right vertical wall was maintained at constant cold temperature and the top wall was considered insulated. They concluded that , non-uniform heating of the bottom wall produced greater heat transfer rate at the center of the bottom wall than the uniform heating case for all Rayleigh numbers, but average Nusselt number showed overall lower heat transfer rate for the non-uniform heating case.

Gustavsen and Thue [11] studied the effect of the horizontal aspect ratio on heat flow through cavities with a high vertical aspect ratio. The cavities studied had two opposite isothermal vertical walls separated by four adiabatic walls. The vertical aspect ratios were 20, 40 and 80 while the horizontal aspect ratios range from 0.2 to 5. The results showed that three-dimensional cavities with a horizontal aspect ratio larger than five can be considered as being two-dimensional cavities to within 4% when considering heat transfer rates.

Mahdi et al. [12] analyzed numerically steady two - dimensional natural convection heat transfer of Newtonian and non-Newtonian fluids inside a square enclosure for a wide range of the modified Rayleigh number of ($10^3 \leq Ra \leq 10^5$) and a modified Prandtl number in the range ( 1,10 and 100).Two types of boundary conditions have been considered; First when the side walls are heated at different uniform temperatures and the horizontal walls are insulated, whereas the second when the

bottom wall was heated by applying a uniform heat flux while the other walls are at a constant cold temperature. The results were presented in terms of isotherms and streamlines to show the behavior of the fluid flow and temperature fields. However, from the above literature review, there were little published researches related with natural convection flow in the cavity filled with water when one of the cavity sidewalls was linearly heated. Most previous studies looked at the influence of Rayleigh number on the flow and thermal fields in closed cavities with constant aspect ratio.

The object of the current study is to solve the steady natural convection flow in a water- filled cavity with various aspect ratios when the bottom wall is maintained at constant hot temperature, the left side wall is linearly heated, the right side wall is considered cold while the top wall is considered adiabatic. The present study is based on the configuration of Sathiyamoorthy et al. [13] where the natural convection flow in a square cavity with linearly heated side wall(s) is studied numerically. Sathiyamoorthy et al. [13] did not investigate the effect of changing the aspect ratio of the cavity on the flow and heat transfer processes. For this reason, it is considered in detail for the first time in the present work.

## PROBLEM DESCRIPTION AND THE MATHEMATICAL ANALYSIS

A problem of two-dimensional, Newtonian, steady, laminar buoyancy-driven flow past a cavity which is filled with water (Pr = 6.0) is formulated mathematically in this section where the Boussinesq approximation is used. This means that all variable-property effects are neglected, except for density in the momentum equation. The configuration is depicted in Fig.1.Cavity aspect ratio (W/H) is varied as 0.5, 1.0 and 2.0 respectively. The aspect ratio is a ratio between the width and the height of the cavity. The left vertical side wall is linearly heated while the right vertical side wall is considered cold. The bottom wall is maintained at constant hot temperature while the top wall is considered adiabatic. The Rayleigh number is varied from $10^3$ to $10^6$ .The governing equations for steady buoyancy-driven flow using conservation of mass, momentum and energy can be written in a dimensionless form as [13]:

$$\frac{\partial U}{\partial X} + \frac{\partial V}{\partial Y} = 0 \tag{1}$$

$$U\frac{\partial U}{\partial X} + V\frac{\partial U}{\partial Y} = -\frac{\partial P}{\partial X} + \Pr\left(\frac{\partial^2 U}{\partial X^2} + \frac{\partial^2 U}{\partial Y^2}\right) \tag{2}$$

$$U\frac{\partial V}{\partial X} + V\frac{\partial V}{\partial Y} = -\frac{\partial P}{\partial Y} + \Pr\left(\frac{\partial^2 V}{\partial X^2} + \frac{\partial^2 V}{\partial Y^2}\right) + Ra\ \Pr\theta \tag{3}$$

$$U\frac{\partial \theta}{\partial X} + V\frac{\partial \theta}{\partial Y} = \left(\frac{\partial^2 \theta}{\partial X^2} + \frac{\partial^2 \theta}{\partial Y^2}\right) \tag{4}$$

These dimensionless governing equations have been obtained by employing the following non-dimensional variables as listed below:

$$X = \frac{x}{H} \quad Y = \frac{y}{H} \quad U = \frac{u\,H}{\alpha} \quad V = \frac{v\,H}{\alpha}$$

$$\theta = \frac{T - T_c}{T_h - T_c} \quad P = \frac{p\,H^2}{\rho\alpha^2} \quad Pr = \frac{\nu}{\alpha} \quad Ra = \frac{g\beta(T_h - T_c)H^3\,Pr}{\nu^2} \tag{5}$$

The non-dimensional boundary conditions are given by:

1- No-slip conditions are applied at all cavity walls, i.e., U = V = 0.
2- The bottom wall of the cavity is maintained at constant hot temperature, i.e., $\theta(X,0) = 1$.
3- The top wall of the cavity is considered adiabatic, i.e., $\frac{\partial\theta}{\partial Y}(X,1) = 0$.
4- The left vertical sidewall of the cavity is linearly heated ,i.e., $\theta(0,Y) = 1 - Y$
5- The right vertical sidewall of the cavity is maintained at constant cold temperature, i.e. $\theta(1,Y) = 0$.

where X and Y are the dimensionless coordinates measured along the horizontal and vertical axes, respectively, u and v being the dimensional velocity components along x and y axes .Also, θ is the dimensionless temperature, P is the dimensionless pressure, Pr is the Prandtl number, Ra is the Rayleigh number, $\beta$ is the volumetric coefficient of thermal expansion, $\rho$ is the density, $\upsilon$ is the kinematic viscosity, $\alpha$ is the thermal diffusivity and g is the gravitational acceleration. The local Nusselt number at the bottom and left sidewalls can be written as [13]:

$$Nu_B = -\left[\frac{\partial\theta}{\partial Y}\right]_{Y=0} \quad and \quad Nu_L = -\left[\frac{\partial\theta}{\partial X}\right]_{X=0} \tag{6}$$

while the average Nusselt number at the bottom and left sidewalls are computed as:

$$\overline{Nu_B} = -\int_0^1 \left[\frac{\partial\theta}{\partial Y}\right]_{Y=0} dX \quad and \quad \overline{Nu_L} = -\int_0^1 \left[\frac{\partial\theta}{\partial X}\right]_{X=0} dY \tag{7}$$

## SOLUTION PROCEDURE AND VERIFICATION

The present computational approach is based on finite volume method to discretize the dimensionless governing equations related to the pressure, temperature and velocities as explained in Colella and Puckett [14]. The computational process of non-uniform grids needs the cell face velocities to be calculated. In the present numerical procedure, the flow inside the cavity is solved with special attention to the corners of the cavity where more girds are clustered in these regions to capture the flow and thermal fields accurately. This is achieved by employing more nodes at the

cavity edges where sharp gradients of velocity and temperature are expected. Figure 2 shows the grid system of the present work.

A FORTRAN program is constructed to compute the pressures, velocities and temperatures. The program runs after introduce the given required data such as Rayleigh number, Prandtl number and an external subroutine is constructed also and linked with the main program to compute the required cavity mesh. After this, the main program begins to discretize the partial differential equations on uniform grids, in which the unknown variable is a dependent function on several variables of space, and to know the evolution of the unknown factor (temperature or velocity) in a finite and homogeneous field starting from known initial values. The obtained tri-diagonal linear systems are solved by the Thomas algorithm approach [15]. The iterative method is used to produce the final results and the iteration process continues until the maximum difference between iterations becomes lower than $10^{-7}$. When, the convergence criterion is satisfied, the output data file is printed. Otherwise, the iteration process still continues to guarantee a satisfactory convergence of the numerical simulation.

In order to verify the present numerical results, a comparison between the results of the present work and the previous results of Sathiyamoorthy et al. [13] is performed for a natural convection simulation in a square cavity (W/H=1) filled with air ( Pr = 0.7) when the left vertical side wall is linearly heated while the right vertical one is maintained at constant cold temperature. This comparison is made for Rayleigh number (Ra = $10^3$ , $10^4$ and $10^5$ ) respectively as shown in Fig. 3.Excellant agreement is achieved between the present work and the work of Sathiyamoorthy et al. [13] for both stream functions and temperatures as shown in Fig. 3 which validates the present computations process.

## RESULTS AND DISCUSSION

The characteristics of the temperature and flow fields in a differentially heated cavity filled with water and have various aspect ratios is examined and discussed in this section. Computations have been carried out for the following ranges of the dimensionless parameters: Prandtl number (Pr) = 6.0**,** the Rayleigh number is varied from $10^3$ to $10^6$, the cavity aspect ratio (W/H) is varied as 0.5, 1 and 2 respectively. The cavity has been analyzed with uniformly heated bottom and non-uniformly heated left sidewalls respectively. While, the right sidewall and the top wall are considered cold and thermally insulated, respectively.

### For Square Cavity

The effect of Rayleigh number variation on natural convection characteristics which is induced by linearly heated left vertical wall in a square cavity (W/H=1) filled with water ( Pr = 6) is displayed in Fig.4 by using streamlines (on the left) and isotherms (on the right) contour for Rayleigh number varying from $10^3$ to $10^6$. The buoyancy-driven flow induced due to the temperature difference between isothermal hot and cold vertical sidewalls which makes the fluid to rotate and transfers the thermal energy from hot left sidewall to cold right sidewall through natural convection

mechanism. The fluid begins to move along the hot bottom wall due to uniform heating effect and then turns smoothly up along the left vertical sidewall due to linear heating effect and then impacts with the adiabatic top wall which causes to turn the flow direction towards the right cold vertical sidewall and turns back horizontally to the central region after hitting the hot bottom wall. As expected due to this repeated fluid movement, re-circulating vortices begin to grow. The circulations are greater near the cavity core and least at the boundaries, due to the no-slip boundary conditions. When the Rayleigh numbers are small ( i.e., Ra = $10^3$ and $10^4$ ) , the buoyancy force effect is slight, so for this case the heat is transferred due to conduction mechanism. The convection role in this case is small because the generated buoyancy force is not high enough to begin fluid convection.

In Figure 4, it is found that when the Rayleigh number is very small ( i.e., Ra = $10^3$ ), the flow field inside the square cavity can be represented by a large singular circular vortex which covers all the cavity size. When the Rayleigh number is slightly increased ( i.e., Ra = $10^4$ ) , the flow field can be represented by a small minor vortex which is located at the left upper corner of the cavity and a large major vortex which occupies the other remaining cavity regions. Furthermore, when the Rayleigh numbers are become large (i.e., Ra = $10^5$ and $10^6$), the minor vortex size increases and the major vortex size decreases, while the shape of the vortices are converted from singular circular shape to non-singular elliptical shape. Furthermore, with the growth of the Rayleigh number, there is a clear growth in the intensity of circulation, since the buoyancy force effect becomes high.

With respect to isotherms, it is found that when the Rayleigh numbers are small (i.e., Ra = $10^3$ and $10^4$), the isotherms are approximately linear and they are symmetrical near the top edges of the cavity sidewalls indicating that the heat is transferred by the conduction. No clear thermal boundary layer can be noticed when the Rayleigh number is small. As the Rayleigh numbers increase (i.e., Ra = $10^5$ and $10^6$), the isotherms are begin to accumulate adjacent to the cavity boundaries indicating that the convection is the dominant mechanism for heat transfer in the cavity. These isotherms refer that a large temperature gradient can be observed there. In this case a thermal boundary layer can be found adjacent to the hot left sidewall and the hot bottom wall of the cavity.

**For Rectangular or Slender Cavity**

The streamline and isotherm contours in a rectangular cavity (W/H=0.5) filled with water (Pr = 6) for linearly heated left vertical sidewall and cold right vertical sidewall with various values of Rayleigh numbers are illustrated in Fig. 5. It is useful to say that, when the aspect ratio is smaller than one (W/H <1), the cavity is called a slender cavity. It is found from this figure, that when the aspect ratio decreases from (W/H=1) in Fig. 4 to (W/H=0.5) in Fig. 5, the convection effect becomes stronger and the circulation strength increases. This is due to the reduction in the cavity width which makes the hot left vertical sidewall closer to the cold right vertical sidewall and as a result causes to increase the convection effect. Also, it can be seen that the re-circulating vortices inside the cavity begin to enlarge in the vertical direction and its shape becomes ellipsoidal. Furthermore, again it can be seen that when the Rayleigh number is very small (i.e., Ra = $10^3$), the flow field can be described by a

large singular vortices which cover all the cavity regions. When the Rayleigh number increases an extra vortices can be observed at the left top zone of the cavity and its size increases as the Rayleigh number increases. With respect to isotherms, when the aspect ratio decreases, the isotherm patterns change significantly especially inside the cavity, indicating that convection is the dominant mechanism for heat transfer in the cavity. The instabilities and disturbance of the isotherm patterns increase with increasing of the Rayleigh number. The isotherms are crowded and pressurized towards the hot bottom wall and left hot sidewall and form a thermal boundary layer.

From this observation it can be concluded that the heat is transferred due to convection when the aspect ratio decreases. However, it can be seen also in the vicinity of the hot bottom wall, hot left and cold right sidewalls that the isotherm patterns are somewhat still linear and parallel. This refers that the conduction is still has a role in the heat transfer mechanism. Moreover, the temperature gradients near both the bottom and left vertical walls play an important role in developing the thermal boundary layer. The linear heating provides a smooth temperature distribution on the cavity boundaries.

**For Shallow Cavity**

The flow and temperature fields in terms of computed streamlines and isotherms in a shallow cavity (W/H = 2) filled with water (Pr = 6) for linearly heated left vertical sidewall and cold right vertical sidewall with various values of Rayleigh numbers are explained in Fig. 6. It is useful to mention that, when the aspect ratio is greater than one (W/H >1), the cavity is called a shallow cavity. It can be seen in Fig. 6, that the flow field can be represented by two major vortices which are distributed to cover all the cavity regions. As the Rayleigh number increases, one of major vortices begins to enlarge while the other vortex begins to diminish. Also, small minor vortices can be noticed near the cavity boundaries. This is can be return to the reduction in the cavity height and increasing in the cavity width which cause the hot left vertical sidewall more far from the cold right vertical sidewall and as a result causes to decrease the convection effect. Also, it can be seen that the re-circulating vortices inside the cavity begin to enlarge in the horizontal direction and its shape becomes irregular. With respect to isotherms, when the aspect ratio increases, the isotherms become in general parallel in shape and approximately linear. Therefore, it can be concluded that the heat is transferred due to conduction when the aspect ratio increases.

**Local Nusselt Number**

Figure 7 demonstrates the variation of local Nusselt number with distance along a hot bottom wall (left) and linearly heated left sidewall (right) for various Rayleigh number and different aspect ratio (W/H= 0.5, 1, 2).For both walls, the local Nusselt number increases when the Rayleigh number increases. For linearly heated left sidewall, the local Nusselt number at this wall ($Nu_L$) is very high especially at the right edge of this wall. This is due to the strong circulations in this region which

causes to increase the temperature gradient and as a result the local Nusselt number increases. Also, It can be seen a strong fluctuations in local Nusselt number behavior with distance along the left sidewall due to non-uniform heating effect at this wall which causes the isotherm contours to be compressed towards the boundary of the cavity and cause this fluctuations. Furthermore, it can be seen that the aspect ratio does not have a significant effect of the local Nusselt number. From the other hand, for hot bottom wall, the local Nusselt number at this wall ($Nu_b$) is again maximum at the right edge of this wall. The physical reason of this behavior is due to the high increase in the temperature gradient and strong circulation which lead to increase the local Nusselt number at this wall. The local Nusselt number decreases at this wall when the aspect ratio increases.

**Average Nusselt Number**

Figure 8 shows variation of average Nusselt number with Rayleigh number along a hot bottom wall (left) and linearly heated left sidewall (right) at different aspect ratio (W/H= 0.5, 1, 2).It can be seen from this figure that for hot bottom wall, when the aspect ratio increases, the average Nusselt number decreases. This is because when the aspect ratio increases, its increasing causes to decrease the cavity height and leads to decrease the Rayleigh number, since this number depends on the cavity height and consequently average Nusselt number decreases. From the other hand, due to non-uniform or linear heating of the left vertical sidewall, the heating rate near this wall is generally high, which induces a high buoyancy effect, resulting in a high thermal gradient and as a result the average Nusselt number increases .Furthermore, it can be seen that as the Rayleigh number increases, the average Nusselt number for both bottom wall and left sidewall increase. This is due to the increase in the convection currents intensity and circulation strength which cause a dramatic increase in the average Nusselt number especially for high Rayleigh number.

## 6. CONCLUSIONS

The following conclusions can be drawn from the results of the present work:

1. When the Rayleigh number is very low ( i.e., Ra = $10^3$ ), the circulation strength is weak and a large singular circular vortex can be observed inside the cavity. At, Ra = $10^4$, the flow field can be represented by a small minor and a large major vortices.

2. With the increasing of Rayleigh number ( i.e., Ra = $10^5$ and $10^6$ ), the major vortex size decreases while the minor vortex size increases and the shape of these vortices become ellipsoidal. Also, a strong circulation can be noticed in the cavity.

3. When the Rayleigh number is low ( i.e., Ra = $10^3$ and $10^4$), the isotherms are in general parallel straight lines adjacent to the left and right cavity sidewalls.

**4.** Sharp thermal boundary layers are found near to the hot left side wall and the hot bottom wall of the cavity and their thickness increase when a Rayleigh number increases.

**5.** For square cavity, when the aspect ratio equals one (W/H = 1), a singular circular vortex is formed. While for slender cavity (W/H <1), the convection effect becomes stronger and the circulation strength increases and the re-circulating vortices inside the cavity begin to enlarge in the vertical direction and its shape becomes ellipsoidal.

**6.** For shallow cavity (W/H >1), the flow field can be represented by two major vortices which are distributed to cover all the cavity regions. As the Rayleigh number increases, one of major vortices begins to enlarge while the other vortex begins to diminish. Also, small minor vortices can be noticed near the cavity boundaries.

**7.** For shallow cavity, the isotherms are usually parallel in shape and approximately linear indicating that the conduction model is dominant. While for slender cavity, the isotherms are non-uniformly and more confusion occurs in it indicating that the convection model is dominant.

**8.** For both hot bottom and left walls, the local Nusselt number increases when the Rayleigh number increases.

**9.** Strong fluctuations occur in local Nusselt number behavior with distance along the left sidewall due to non-uniform heating effect at this wall.

**10.** For linearly heated left sidewall, the aspect ratio does not have a significant effect of the local Nusselt number, while for hot bottom wall the local Nusselt number decreases when the aspect ratio increases.

**11.** For hot bottom wall, the average Nusselt number decreases when the aspect ratio increases.

**12.** For hot left vertical sidewall, the average Nusselt number increases when the aspect ratio increases due to non-uniform or linear heating at this wall.

**13.** For both left side and bottom walls the average Nusselt number increase with the Rayleigh number.

## REFERENCES

[1] Baytas, A., "Buoyancy-driven flow in an enclosure containing time periodic internal sources", Heat and Mass Transfer, Vol.31, pp: 113 –119, (1996).

[2] Imberger, J., "Natural convection in a shallow cavity with differentially heated end walls. Part 3 : Experimental results", J. Fluid Mech., Vol. 65, No. 2, pp: 247–260, (1974).

[3] Hasnaoui, M., Bilgen , E. and Vasseurt, P., "Natural convection heat transfer in rectangular cavities partially heated from below", J. of Thermophysics and Heat Transfer, Vol. 6, No. 2, pp : 255 –265, (1992).

[4] Braunsfurth, M., Skeldon, A., Juel, A., Mullin, T. and Riley, D.,"Free convection in liquid gallium", J. Fluid Mech., Vol. 342, pp.: 295–314, (1997).

[5] Aydin, O. and Yang, W.,"Natural convection in enclosures with localized heating from below and symmetrical cooling from sides", Int. J. of Numerical Methods for Heat and Fluid Flow, Vol. 10, No.5, pp: 518 – 529, (2000).

[6] Kalita, J., Dalal, D. and Dass, A., "Fully compact higher-order computation of steady-state natural convection in a square cavity", Physical Review E, Vol. 64, pp: 1-13, (2001).

[7] Basak, T., Roy, S. and Balakrishnan, A., "Effects of thermal boundary conditions on natural convection flows within a square cavity", Int. J. of Heat and Mass Transfer, Vol.49, pp: 4525–4535, (2006).

[8] Xin, S. and Quere, P., "Natural convection flows in air-filled,differentially heated cavities with adiabatic horizontal walls", Numerical Heat Transfer, Part A ,Vol. 50, pp : 437–466, (2006).

[9] Mariania, V. and Belo, I., "Numerical studies of natural convection in a square cavity", Engenharia Termica (Thermal Engineering), Vol. 5, No.1, pp : 68-72, (2006).

[10] Basak, T., Roy, S. and Takhar, H., "Effects of non-uniformly heated wall(s) on a natural convection flow in a square cavity filled with a porous medium", Numerical Heat Transfer , Part A ,Vol. 51, pp : 959–978, (2007).

[11] Gustavsen, A. and Thue, J., "Numerical simulation of natural convection in three-dimensional cavities with a high vertical aspect ratio and a low horizontal aspect ratio", Journal of Building Physics, Vol. 30, pp : 217–240 (2007).

[12] Mahdi, A., Hussian, T. and Jassim, N., "Laminar natural convection of Newtonian and Non – Newtonian fluids in a square enclosure", Engineering and Technology Journal, Vol. 26, No.1, pp:74–91, (2008).

[13] Sathiyamoorthy, M., Basak, T., Roy, S. and Pop, I., "Steady natural convection flows in a square cavity with linearly heated side wall(s), Int. J. Heat and Mass Transfer, Vol. 50, pp :766–775, (2007).

[14] Colella, P. and Puckett, E., "Modern Numerical Methods for Fluid Flow", University of California, U.S.A. (1994).

[15] Tannehill, J., Anderson, D. and Fletcher, R., "Computational fluid mechanics and heat transfer", Taylor and Francis, Washington, U.S.A., (1997).

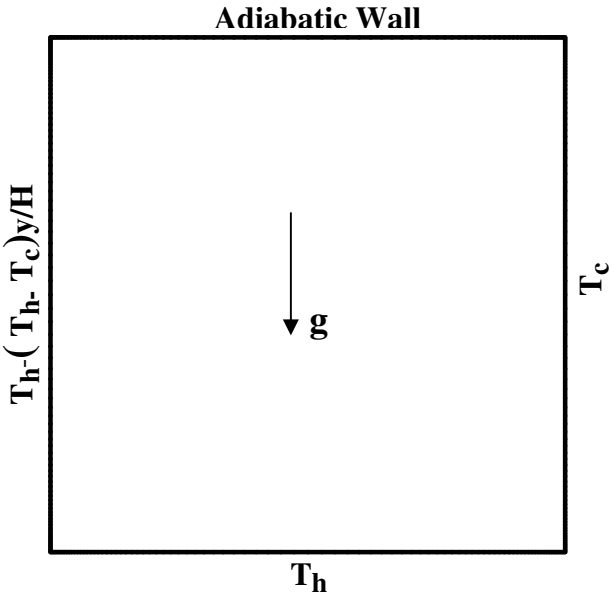


**Fig.1**. Schematic diagram of the square cavity (W/H=1) filled with water at coordinate system along with boundary conditions.

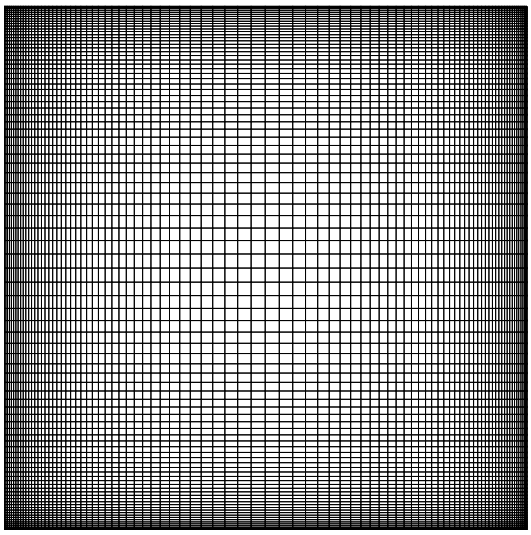

**Fig. 2.** A typical 2D - grid distribution (88 x 88) with non-uniform and orthogonal distributions for the square cavity

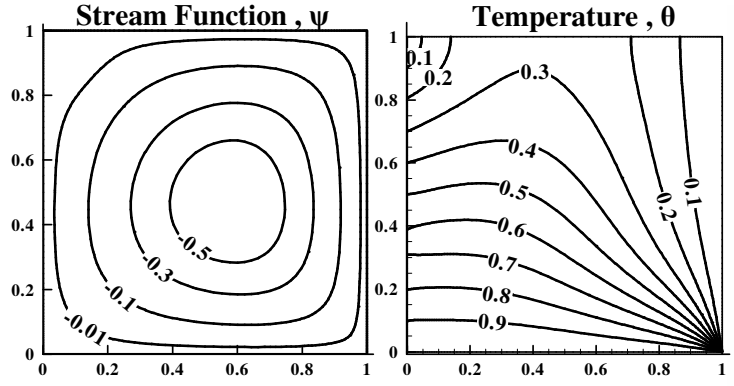


*a. Ra=10³*

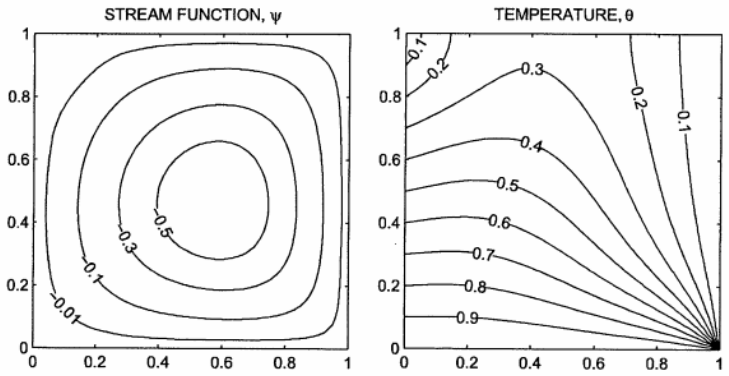


*a. Ra=10³*

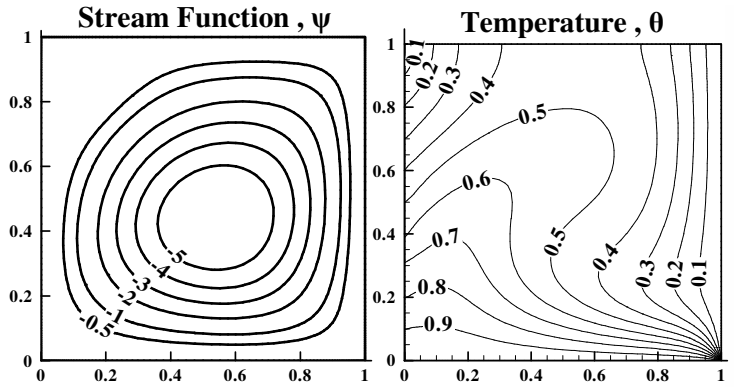


*b. Ra=10⁴*

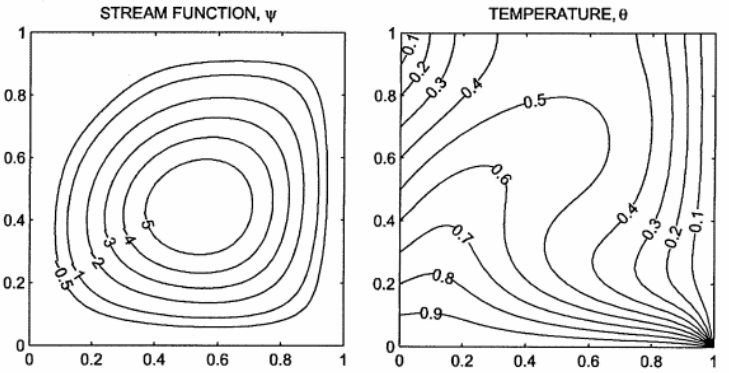


*b. Ra=10⁴*

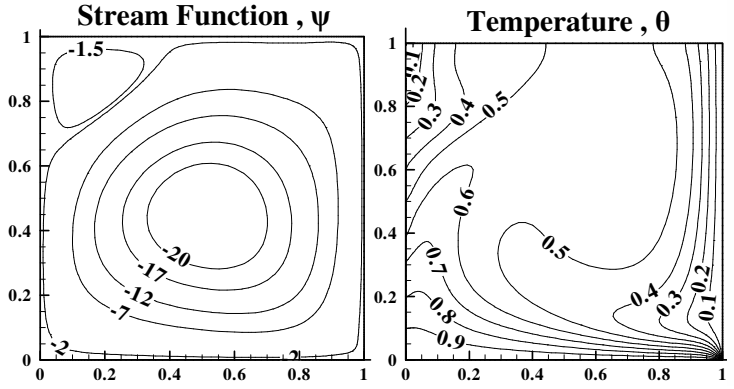


*c. Ra=10⁵*

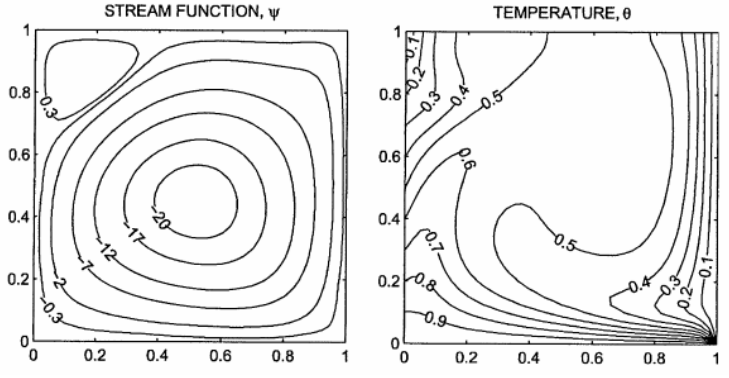


*c. Ra=10⁵*

**Present Results** **Sathiyamoorthy et al. Results [13]**

**Fig.3.** Comparison of the streamline and isotherm contours between the present work and that of Sathiyamoorthy et al. [13] in a square cavity (W/H=1) filled with air (Pr = 0.7) for linearly heated left sidewall and cold right sidewall with various values of Rayleigh numbers.

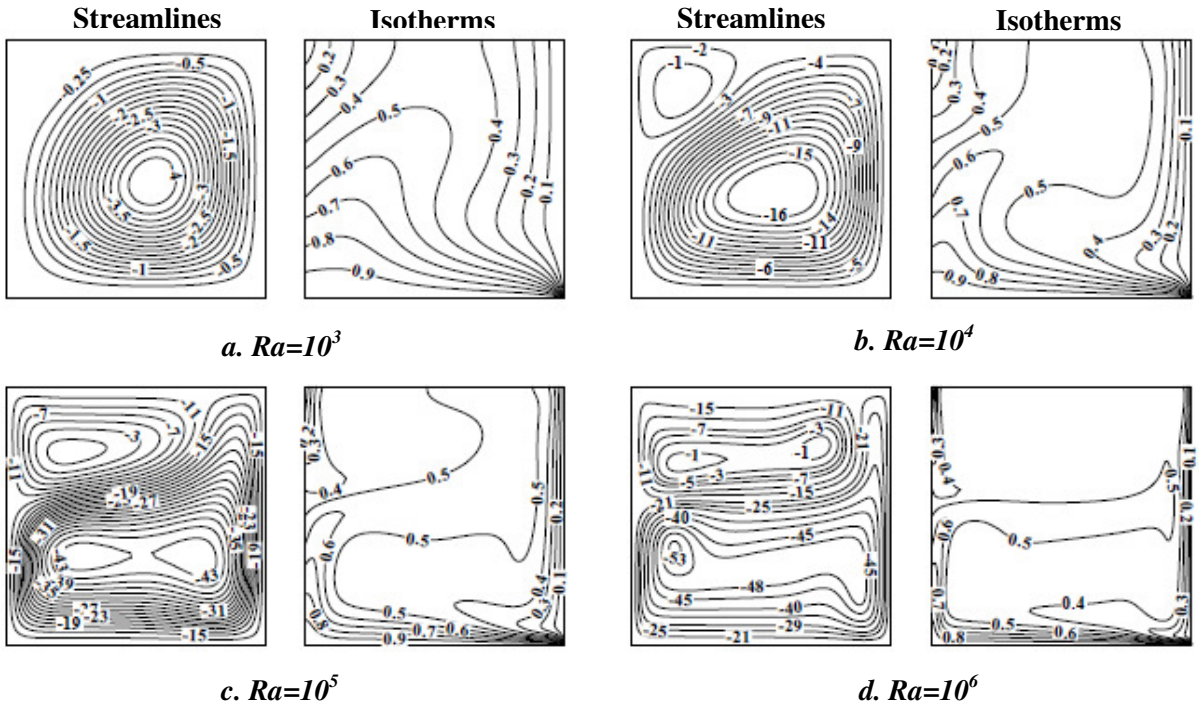


**Fig.4.** Streamline and isotherm contours in a square cavity (W/H=1) filled with water (Pr = 6) for linearly heated left sidewall and cold right sidewall with various values of Rayleigh numbers.

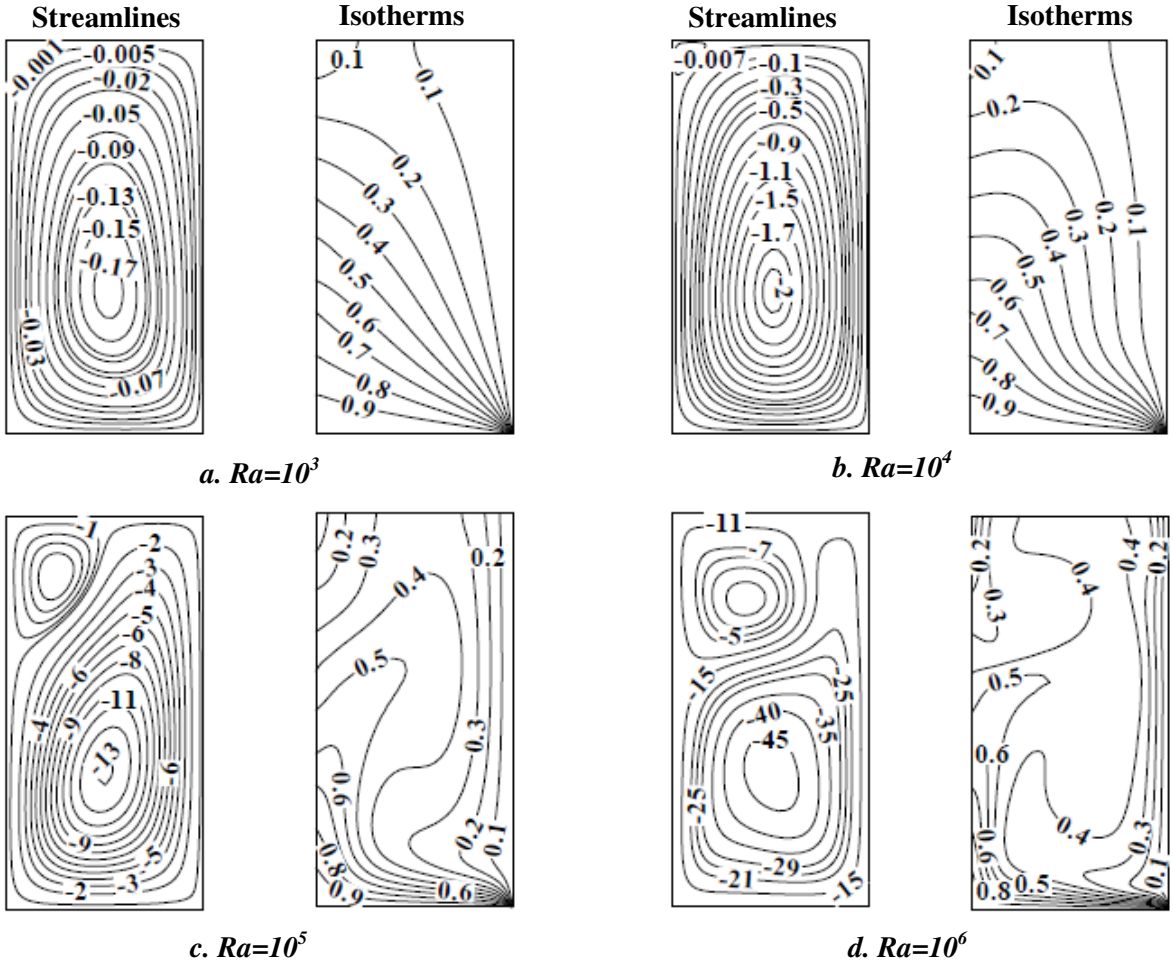


**Fig.5.** Streamline and isotherm contours in a slender cavity (W/H= 0.5) filled with water (Pr = 6) for linearly heated left sidewall and cold right sidewall with various values of Rayleigh numbers.

**Streamlines** **Isotherms**

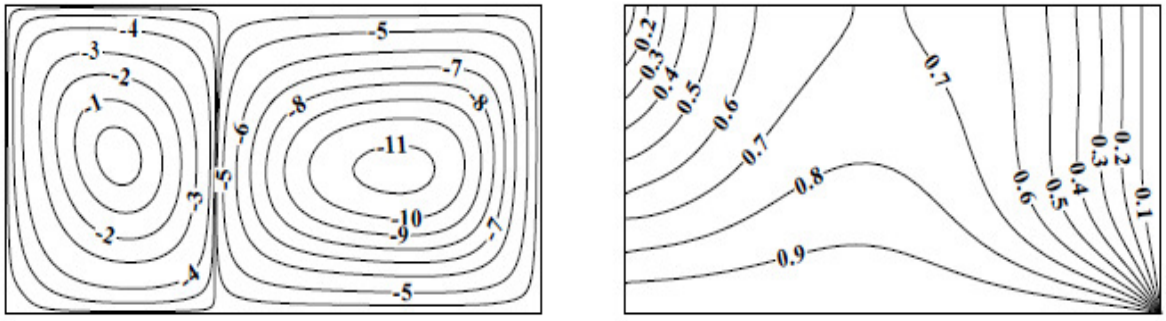

***a. Ra=10^3***

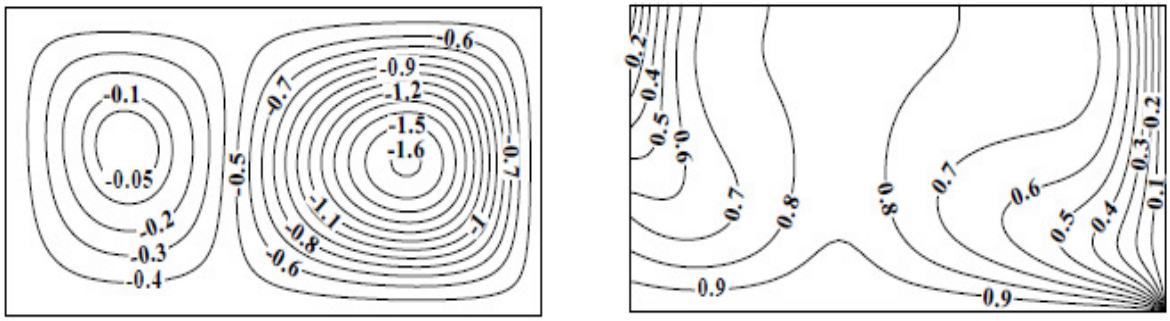

***b. Ra=10^4***

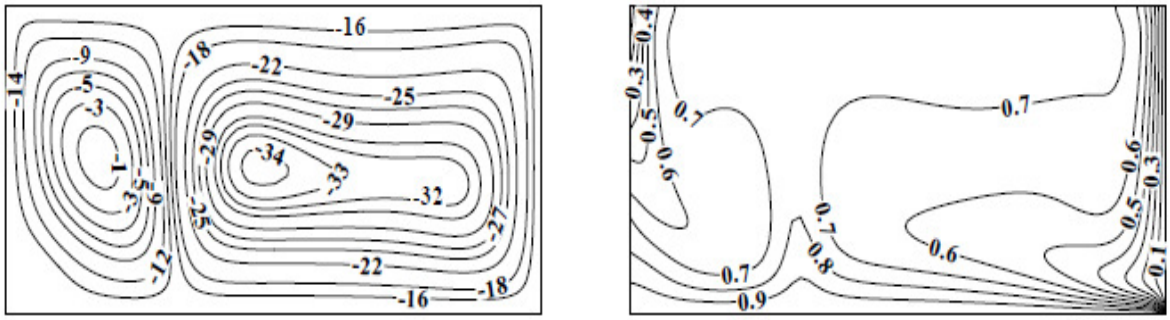

***c. Ra=10^5***

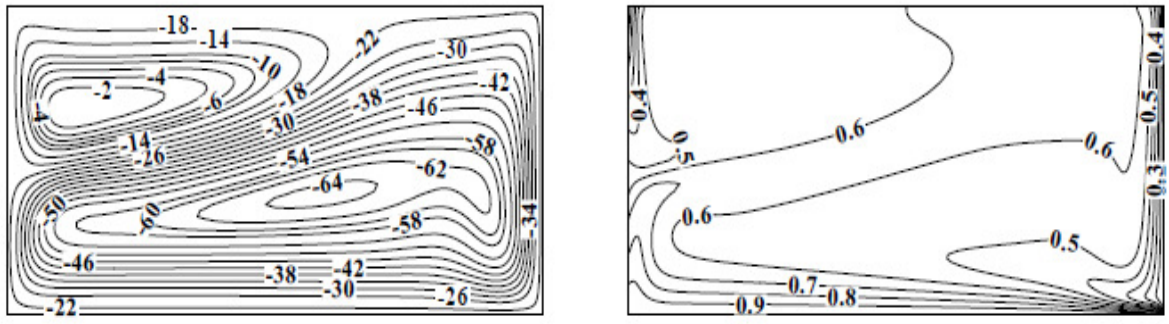

***d. Ra=10^6***

**Fig.6.** Streamline and isotherm contours in a shallow cavity (W/H= 2) filled with water (Pr = 6) for linearly heated left sidewall and cold right sidewall with various values of Rayleigh numbers.

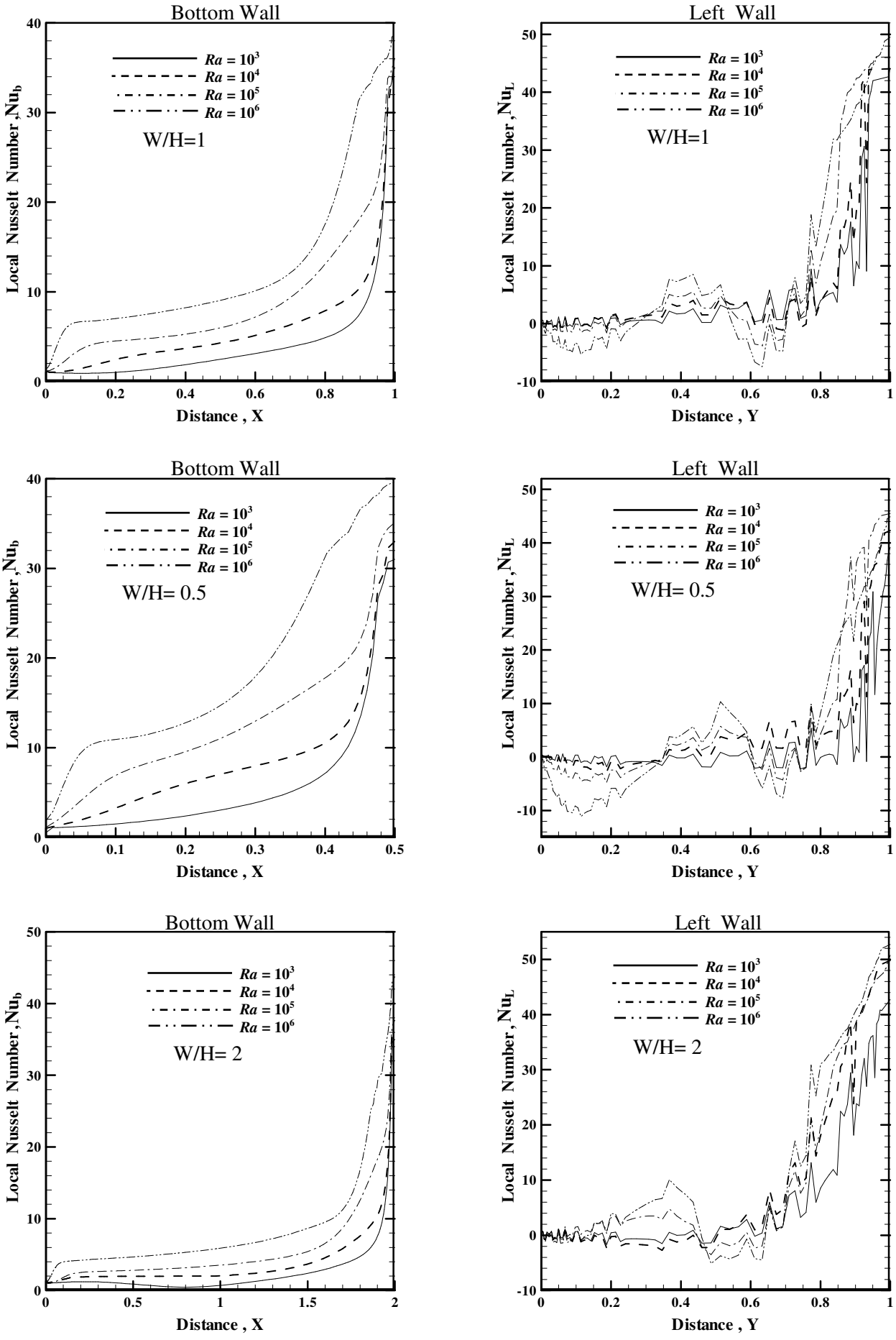


**Fig.7.**Variation of local Nusselt number with distance along a hot bottom wall (on the left) and linearly heated left sidewall (on the right) for various Rayleigh number and different aspect ratios (W/H= 0.5, 1, 2).

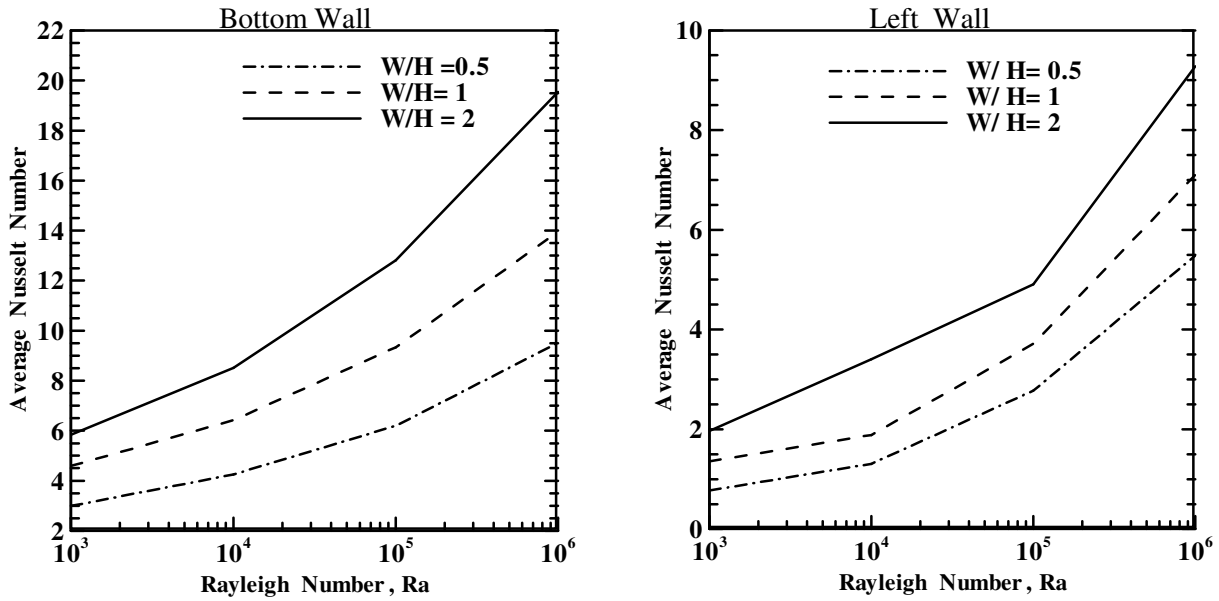


**Fig.8.** Variation of average Nusselt number with Rayleigh number along a hot bottom wall (on the left) and linearly heated left sidewall (on the right) at different aspect ratios (W/H = 0.5, 1, 2).